Journal of Technomaterial Physics
Journal homepage: https://talenta.usu.ac.id/JoTP

Entrance Surface Air Kerma (ESAK) in Adult Posteroanterior (PA) Chest Radiography: An Exploratory Analysis

Intan Mulia Sari*, Irhamni, Rini Safitri, Evi Yufita, and Ariana Shafira Dewi
Department of Physics, Faculty of Mathematics and Natural Sciences, Universitas Syiah Kuala, Aceh 23111, Indonesia
*Corresponding Author: ms.intan@usk.ac.id

ARTICLE INFO

Article history:
Received 24 January 2026
Revised 04 March 2026
Accepted 08 March 2026
Available online 10 March 2026

E-ISSN: 2656-0755
P-ISSN: 2656-0747

How to cite:
I. M. Sari, Irhamni, R. Safitri, E. Yufita, and A. S. Dewi, "Entrance Surface Air Kerma (ESAK) in Adult Posteroanterior (PA) Chest Radiography: An Exploratory Analysis," Journal of Technomaterial Physics, vol. 08, no. 01, pp. 20-29, Feb. 2026, doi: 10.32734/jotp.v8i1.24603.

ABSTRACT

This study estimated Entrance Surface Air Kerma (ESAK) for adult posteroanterior (PA) chest radiography and described ESAK patterns in relation to selected technical parameters and patient characteristics as an initial facility-level baseline. A descriptive–exploratory observational study was conducted in 10 adult patients using a Siemens digital radiography system equipped with Automatic Exposure Control (AEC). ESAK was estimated from X-ray tube output obtained from acceptance/constancy testing and combined with routinely recorded exposure parameters. Incident air kerma (INAK) was calculated first and then converted to ESAK using a backscatter factor assumed to be constant at 1.35. All examinations were performed at 125 kVp with a fixed source-to-image distance (SID) of 180 cm. Focus-to-skin distance (FSD) was not recorded directly and was estimated from SID and the recorded chest thickness. ESAK ranged from 0.09 to 0.17 mGy (mean, 0.13 mGy), and all values were below the BAPETEN optimization reference level of 0.2 mGy. In this limited sample, graphical patterns indicated that ESAK increased with mAs and body weight and decreased with increasing FSD. These findings are preliminary and require confirmation in a larger cohort; however, they may serve as a temporary local baseline for internal dose auditing and to inform the design of subsequent dose optimization studies.

Keywords: Chest Radiography, Dose Optimization, ESAK, Patient Dose, Radiation Protection

ABSTRAK

Penelitian ini mengestimasi *Entrance Surface Air Kerma* (ESAK) pada radiografi toraks dewasa proyeksi *posteroanterior* (PA) dan mendeskripsikan pola nilai ESAK terhadap parameter teknik serta karakteristik pasien sebagai data awal tingkat fasilitas. Studi observasional deskriptif–eksploratif dilakukan pada 10 pasien dewasa menggunakan sistem radiografi digital Siemens dengan *Automatic Exposure Control* (AEC). ESAK diestimasi dari keluaran tabung sinar-X hasil uji kesesuaian dan parameter paparan rutin. *Incident air kerma* (INAK) dihitung terlebih dahulu, kemudian dikonversi menjadi ESAK menggunakan faktor hambur balik yang diasumsikan konstan sebesar 1,35. Pemeriksaan dilakukan pada 125 kVp dengan *source-to-image distance* (SID) 180 cm. *Focus-to-skin distance* (FSD) tidak dicatat langsung dan diestimasi dari SID serta ketebalan toraks. ESAK berkisar 0,09–0,17 mGy dengan rerata 0,13 mGy, dan seluruh nilai berada di bawah acuan optimisasi BAPETEN 0,2 mGy. Pada sampel terbatas ini, pola pada grafik menunjukkan ESAK meningkat seiring mAs dan berat badan, serta menurun dengan meningkatnya FSD. Temuan ini bersifat awal dan memerlukan konfirmasi pada kohort yang lebih besar, namun dapat digunakan sebagai nilai acuan lokal sementara untuk audit dosis internal dan perencanaan studi optimisasi dosis berikutnya.

Kata kunci: Dosis Pasien, ESAK, Optimisasi Dosis, Proteksi Radiasi, Radiografi Toraks

http://doi.org/10.32734/jotp.v8i1.24603

1. Introduction

The use of ionizing radiation is an integral part of modern medical practice, particularly in diagnostic and interventional radiology to support clinical decision-making. Conventional radiographic X-ray systems remain among the most widely used sources of medical ionizing radiation, in which X-rays are generated when high-energy electrons emitted from the cathode are accelerated toward an anode target under an applied potential difference, typically in the range of 20–150 kVp [1]. The resulting X-ray beam penetrates patient tissues and is detected by an image receptor to form a radiographic image.

Among conventional radiographic procedures, posteroanterior (PA) chest radiography is one of the most frequently performed examinations in healthcare facilities. It plays an important clinical role in evaluating the lungs, heart, and other thoracic structures for screening and diagnostic purposes. Although the dose per chest radiograph is generally lower than that of modalities such as computed tomography (CT) [2], the high volume of examinations and variations in local practice make patient dose optimization in chest radiography a relevant topic in medical physics and radiation protection [3].

Medical exposure to ionizing radiation carries a potential risk of stochastic effects; therefore, the implementation of radiation protection principles is essential. In Indonesia, patient radiation protection and safety for X-ray utilization are regulated by the Nuclear Energy Regulatory Agency (Badan Pengawas Tenaga Nuklir, BAPETEN), including provisions that emphasize monitoring and control of patient doses as part of a radiation safety assurance system [4]. These requirements are consistent with international recommendations from the International Commission on Radiological Protection (ICRP) [5] and the International Atomic Energy Agency (IAEA) [6], which emphasize the principles of justification and optimization according to the As Low As Reasonably Achievable (ALARA) concept.

In the context of optimization, patient dose audits using standardized dosimetric quantities are widely used to evaluate exposure practices and to identify areas for protocol improvement. In digital radiography, several dose-related metrics—such as entrance surface air kerma (ESAK) and kerma–area product (KAP)—are commonly applied for patient dose monitoring, performance evaluation, and as supporting inputs in establishing local diagnostic reference levels (local DRLs) [7]. ESAK is defined as the air kerma at the patient entrance surface including the contribution of backscattered radiation, and it may be estimated using measured X-ray tube output combined with clinical exposure parameters and appropriate geometric corrections [8].

Previous studies have reported that ESAK or entrance skin dose (ESD) for adult PA chest radiography can vary substantially between facilities and across countries. Such variability is often associated with differences in exposure technique, imaging system characteristics, examination geometry, and the implementation level of quality control programs. For example, relatively low ESAK values on the order of 0.1 mGy have been reported in adult PA chest radiography using digital radiography systems in Thailand [9], while studies in Tanzania have demonstrated broader dose variations across digital radiographic examinations, suggesting further potential for optimization [10].

From a physics and dosimetry perspective, ESAK in radiographic examinations is primarily influenced by exposure parameters and geometry, particularly tube voltage (kVp), tube current–time product (mAs), filtration, collimation (field size), and focus-to-skin distance (FSD) [5,11]. These parameters jointly determine the quantity and quality of the X-ray beam and therefore affect the patient dose. Accurate estimation of tube output and subsequent ESAK calculation require calibrated dosimetry to ensure measurement reliability. In digital radiography, exposure indicators such as the Deviation Index (DI) can support exposure consistency as part of quality assurance programs, helping maintain an appropriate balance between image quality and patient dose [12].

In addition to technical factors, patient-related characteristics may contribute to dose variability because they influence beam attenuation and automatic exposure control (AEC) behavior in clinical practice. Several studies in Indonesia have reported associations between ESAK and technical parameters as well as basic patient characteristics such as body mass and age [13–14]. These findings support the importance of developing local dosimetric datasets that can inform dose monitoring and facilitate the establishment of local DRLs used as optimization benchmarks within facility-level radiation protection programs [15]. Importantly, DRLs (or related reference levels) are intended as tools for optimization and investigation when values are consistently higher than expected, rather than as strict individual dose limits.

Nevertheless, the adoption of digital radiography introduces specific challenges, including exposure creep, which refers to a gradual and often unnoticed increase in exposure over time. Due to the wide dynamic range of digital systems, images may remain diagnostically acceptable even when exposures exceed what is necessary. Without systematic monitoring and feedback through quality assurance, this may lead to unnecessary increases in patient dose. Accordingly, many studies emphasize the need for routine monitoring

of exposure indicators and dose-related metrics to control exposure variability and support continuous optimization [16].

This study presents a facility-based pilot dose audit for adult PA chest radiography by estimating ESAK from routinely recorded exposure parameters used in daily clinical practice. The objectives are (1) to estimate ESAK in adult PA chest radiography at a healthcare facility in Banda Aceh using routine exposure parameters (kVp, mAs, and FSD), and (2) to describe patterns between ESAK and key technical parameters and basic patient characteristics within the observed sample. Given the limited sample size (n = 10), the analyses are intended to be descriptive and exploratory rather than for strong statistical inference or broad generalization. The results are expected to provide pilot data to inform the planning of routine dose monitoring, dose audits, and future optimization studies with larger patient cohorts [17].

2. Methods

2.1. Research Design

This study employed an observational, quantitative, descriptive–exploratory pilot design. The primary objective was to estimate Entrance Surface Air Kerma (ESAK) for adult posteroanterior (PA) chest radiography under routine clinical practice at a single facility. A secondary objective was to describe exploratory patterns between ESAK and selected technical parameters and basic patient characteristics.

Because the sample size was limited (n = 10), all analyses were intended to be descriptive and exploratory, not for population-level inference, causal conclusions, or broad generalization. No changes were made to clinical protocols; therefore, the dataset reflects routine radiographic practice.

2.2. Place and Time

The study was conducted in the radiology department of a healthcare facility in Banda Aceh City using a Siemens digital radiography X-ray system. Data were collected retrospectively from examinations performed between January and February 2024, during which the facility's adult PA chest protocol remained unchanged.

2.3. Subjects and Eligibility Criteria

Records were selected purposively based on completeness and conformity to the standard adult PA chest protocol. Inclusion criteria were:

a) adult patients aged 30–60 years,
b) standard PA chest radiography performed using Automatic Exposure Control (AEC),
c) availability of complete records for sex, age, body weight, chest thickness, and exposure/geometry parameters (kVp, mAs, and SID).

Examinations were excluded if records were incomplete, if the projection was not standard PA chest, or if examinations involved special conditions such as repeat exposures or additional projections. Based on these criteria, 10 examinations were eligible and included.

2.4. Variables and Data Sources

For each included examination, the following data were extracted from routine radiography records:

a) Patient characteristics: age (years), body weight, BW (kg), and chest thickness (cm).
b) Exposure/geometry parameters: tube voltage (kVp), tube current–time product (mAs), and source-to-image distance (SID).

The facility's standard adult PA chest protocol used 125 kVp and SID = 180 cm (fixed by protocol). Therefore, the primary sources of variation across patients were mAs (AEC response) and estimated FSD (from chest thickness).

2.5. Geometry and Estimation of Focus-to-Skin Distance (FSD)

Patient-specific focus-to-skin distance (FSD) was not recorded directly; therefore, it was estimated using examination geometry. Chest thickness was measured as anteroposterior thickness in the PA position using a patient thickness caliper at the mid sternum or nipple line level, with the patient standing with the anterior chest against the bucky at full inspiration, and recorded in centimeters. Under PA chest positioning with the patient close to the image receptor, the object-to-detector distance can be approximated by the recorded chest thickness T (cm). Thus, FSD was estimated as [18]:

$$FSD = SID - T \tag{1}$$

where, SID is the source-to-image distance (cm), fixed at 180 cm, T is the recorded chest thickness (cm).

This approach yields patient-specific FSD values (as shown in the dataset/table 1) and is suitable for a pilot audit. Any residual gap between the patient and the detector (e.g., incomplete contact with the bucky) may

cause the estimated FSD to differ from the true FSD; this is treated as a source of systematic uncertainty.

2.6. Dose Quantities and Calculation

Definitions

$K_a(d)$: free-in-air air kerma at a reference distance d from the X-ray tube (no backscatter).

$Y(d, kVp)$: tube output at distance d for a given tube voltage (mGy/mAs), obtained from calibrated output data.

$K_{a,i}$ (INAK) : incident air kerma at the patient entrance surface (free-in-air at the skin, without backscatter).

$K_{a,e}$ (ESAK): entrance surface air kerma including backscatter.

BSF : backscatter factor.

Free-in-air air kerma at reference distance

Free-in-air air kerma at the reference distance d was obtained from the tube output and the recorded mAs [18]:

$$K_a(d) = Y(d, kVp) \times mAs \tag{2}$$

Because the protocol used a fixed tube voltage (125 kVp), the tube output $Y(d, kVp)$ was taken from quality control measurements. Output was measured using a calibrated dosimeter at d = 100 cm, 125 kVp, and 10×10 cm field size. The mean output obtained was Output_100 = 0.05514 mGy/mAs, and this value was applied consistently in Eq. (2).

Incident air kerma at the patient entrance surface

The kerma at the patient entrance surface was calculated by applying inverse square correction from the reference distance d to the estimated patient-specific FSD [18]:

$$K_{a,i} = K_a(d) \times \left(\frac{d}{FSD}\right)^2 \tag{3}$$

This step accounts for differences in patient positioning/size through FSD.

Entrance Surface Air Kerma including backscatter (ESAK)

ESAK was estimated by applying a backscatter factor [18]:

$$K_{a,e} = K_{a,i} \times BSF$$

$$ESAK = INAK \times 1.35 \tag{4}$$

In this pilot study, BSF was assumed constant at 1.35 as a representative value for adult chest radiography at high kVp. This approximation was used because examination-specific parameters influencing BSF (e.g., field size/collimation and HVL/filtration) were not fully available from routine records. The use of constant BSF is therefore considered a limitation and a source of systematic uncertainty [14, 15, 18].

2.7. Data Processing and Statistical Analysis

INAK ($K_{a,i}$) and ESAK ($K_{a,e}$) were summarized using descriptive statistics. Central tendency was reported as mean and minimum–maximum range. To provide an optimization-oriented context, ESAK values were compared with the reference level stated in BAPETEN guidance (0.2 mGy). Results were categorized as [19]:

- at or below the reference level ($ESAK \leq 0.2$ mGy), and
- above the reference level ($ESAK > 0.2$ mGy).

This comparison is intended to support dose auditing and optimization discussion and should not be interpreted as an individual patient dose limit.

Exploratory relationships between ESAK and selected variables (mAs, estimated FSD, and BW) were evaluated using scatter plots and Pearson correlation coefficients to describe linear association:

$$r = \frac{n(\sum XY) - (\sum X)(\sum Y)}{\sqrt{[n\sum X^2 - (\sum X)^2][n\sum Y^2 - (\sum Y)^2]}} \tag{5}$$

Given that ESAK is mathematically derived from mAs and FSD through Eqs. (2)–(4), any strong association between ESAK and mAs/FSD is expected and is interpreted primarily as a consistency/sensitivity reflection of the calculation model under routine practice, rather than as independent causal evidence. For BW, any observed pattern is interpreted cautiously because BW is an indirect surrogate for attenuation and may not fully capture positioning and thickness distribution. With n = 10, all relationship analyses are descriptive–exploratory.

3. Results and Discussions

This study provides a facility-based, descriptive–exploratory evaluation of 10 adult posteroanterior (PA) chest radiographic examinations performed under routine clinical practice. Patient-related variables included sex, age, body weight, and recorded chest thickness. Technical variables comprised tube voltage (kVp), tube current–time product (mAs) selected by Automatic Exposure Control (AEC), and source-to-image distance (SID). Focus-to-skin distance (FSD) was not measured directly; it was estimated from the fixed SID (180 cm) and recorded chest thickness using Equation (1), as described in the Methods. Dosimetric quantities included incident air kerma (INAK) and entrance surface air kerma (ESAK).

All examinations were performed using a constant tube voltage of 125 kVp and a fixed SID of 180 cm. Maintaining constant kVp is important because changes in kVp alter beam quality and tube output, which would confound comparisons of estimated dose between examinations. Under this standardized protocol, the observed variability in INAK and ESAK across patients is consistent with differences in AEC-selected mAs (reflecting attenuation differences) and small variations in estimated FSD arising from recorded chest thickness. Importantly, because ESAK is calculated from mAs and FSD (via inverse square correction and backscatter correction), strong numerical associations between ESAK and these variables are expected and should be interpreted primarily as a consistency/sensitivity reflection of the calculation model under routine practice rather than as evidence of independent causal relationships.

3.1. Patient characteristics, Exposure Parameters, and Estimated Doses

Table 1 presents individual patient data, exposure parameters, and derived dose quantities. With kVp (125) and SID (180 cm) fixed, mAs ranged from 3.17 to 5.63 mAs, chest thickness ranged from 18.8 to 23.8 cm, and estimated FSD ranged from 161.2 to 156.2 cm.

Table 1. Patient data, exposure parameters, and dosimetric outputs.

No	Age (years)	Body Weight (kg)	Chest Thickness (cm)	kVp	mAs	SID (cm)	FSD (cm)	INAK $K_{a,i}$ (mGy)	ESAK $K_{a,e}$ (mGy)
1	50	48	18.8	125	3.17	180	161.2	0.067	0.091
2	30	53	19.8	125	3.66	180	160.2	0.079	0.106
3	39	54	19.8	125	3.69	180	160.2	0.079	0.106
4	42	56	20.4	125	3.96	180	159.6	0.086	0.116
5	52	59	21.0	125	4.25	180	159.0	0.093	0.125
6	54	62	21.6	125	4.55	180	158.4	0.100	0.135
7	57	65	22.0	125	4.75	180	158.0	0.105	0.141
8	44	68	22.6	125	5.04	180	157.4	0.112	0.151
9	60	72	23.4	125	5.43	180	156.6	0.122	0.165
10	48	74	23.8	125	5.63	180	156.2	0.127	0.171

Across this sample, greater recorded chest thickness generally coincided with higher mAs selected by the AEC and higher INAK/ESAK values, which is consistent with the expected behavior of AEC systems compensating for increased attenuation to maintain detector exposure [5].

A summary of patient characteristics and dose estimates is shown in Table 2. The sample comprised adults aged 30–60 years (mean 47.6 years). Body weight ranged from 48 to 74 kg (mean 61.1 kg), and chest thickness ranged from 18.8 to 23.8 cm (mean 21.3 cm). INAK ranged from 0.07 to 0.13 mGy, while ESAK ranged from 0.09 to 0.17 mGy.

Table 2. Patient data for PA chest radiographic examinations.

Number of Patients		Age (years) Range/ Mean	Body Weight (kg) Range/ Mean	Chest Thickness (cm) Range/ Mean	kVp	mAs (Range/ Mean)	FSD (cm) Range/ Mean	Patient Dose (mGy) Range/Mean		BAPETEN Reference Level (mGy)	
M	F							$K_{a,i}$	$K_{a,e}$	$K_{a,i}$	$K_{a,e}$
3	7	30-60/ 47.6	48-74/ 61.1	18.8-23.8/ 21.3	125	3.2-5.6/ 4.4	156.2-161.2/ 158.7	0.07-0.13/ 0.09	0.09-0.17/ 0.13	0.2	0.2

The systematic finding that ESAK exceeds INAK is expected because ESAK incorporates the contribution of backscattered radiation at the entrance surface through the backscatter factor (BSF). In contrast, INAK represents the incident component without backscatter. Therefore, with BSF > 1, ESAK must be higher than INAK by definition. This indicates internal consistency of the dose calculation workflow used in this pilot dataset and aligns with standard dosimetric practice and guidance [5, 20].

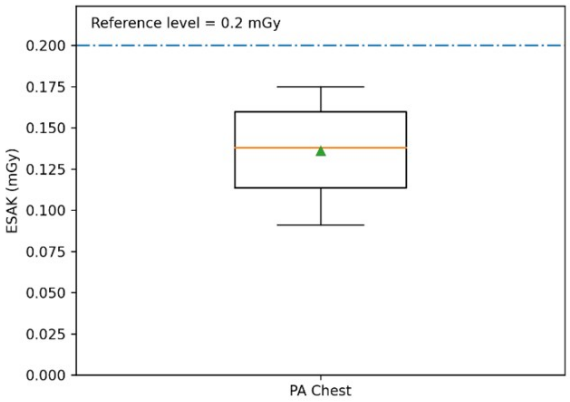

Figure 1. Distribution of Entrance Surface Air Kerma (ESAK) values in posteroanterior (PA) chest radiography.

The distribution of ESAK values is shown in Figure 1. Even with fixed kVp and SID, dose variability remains across patients. Presenting the distribution is useful for dose auditing because it highlights not only the mean ESAK but also the inter-patient spread. For facility-based optimization, inter-patient variability may reflect differences in patient attenuation (thickness/habitus), positioning geometry (estimated FSD), and AEC-selected mAs. In this pilot dataset, ESAK values remained below 0.2 mGy [19]; however, given the small sample size, this should be interpreted as an initial baseline rather than a definitive facility-wide conclusion.

3.2. Relationship between ESAK and mAs

The relationship between ESAK and mAs is shown in Figure 2. A linear fit within this limited dataset yielded:

$$ESAK = 0.0329 \cdot \text{mAs} - 0.0143 \quad (6)$$

with high goodness-of-fit values (reported R^2 and r). However, these very high values should be interpreted cautiously. In this study, ESAK is calculated from tube output multiplied by mAs (and corrected for distance and backscatter). Therefore, a near-linear relationship between ESAK and mAs is expected by construction, particularly when kVp is held constant and other sources of variation are modest. In this context, the fitted slope can be viewed as an empirical sensitivity over the observed mAs range (3.2–5.6 mAs) rather than as evidence of a new causal relationship. The negative intercept should not be interpreted physically; it is a model artifact resulting from fitting a line over a narrow range and does not imply meaningful ESAK values at very low mAs.

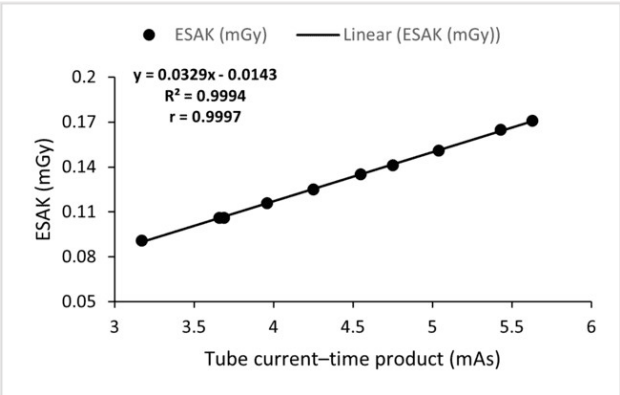

Figure 2. Correlation between ESAK and mAs.

With tube voltage kept constant, changes in mAs primarily modify the quantity of the X ray beam, namely the number of photons produced by electron interactions at the anode target. Because beam quality is largely determined by kVp, maintaining a fixed kVp keeps the energy spectrum relatively unchanged, so an increase in mAs mainly raises beam intensity and the air kerma delivered to the patient entrance surface. From a dosimetric standpoint, this explains why ESAK tends to increase as mAs increases in PA chest radiography performed at constant kVp [1, 18].

In examinations using Automatic Exposure Control, mAs is an output adjusted by the system to maintain the detector exposure at a target level. When patient attenuation is higher, the system tends to select a higher mAs to preserve image quality, which can lead to a higher ESAK. Because ESAK is estimated from exposure parameters that include mAs, the ESAK and mAs relationship observed in this study is best understood as an expected pattern arising from basic X ray beam physics and AEC behavior in routine practice, rather than as independent causal evidence. Future studies with larger samples and additional recorded parameters (e.g., collimation/field size, grid use, AEC chamber selection, and exposure index) would enable more detailed assessment of how each factor contributes to dose variability beyond what is mathematically imposed by the calculation model.

3.3. Relationship between ESAK and FSD

The relationship between ESAK and focus to skin distance (FSD) is shown in Figure 3. A linear fit within this limited dataset yielded:

$$ESAK = -0.01611 \cdot \mathrm{FSD} + 2.68730 \quad (7)$$

A linear regression over the observed range indicates a strong negative association (high reported R^2 and r), meaning ESAK decreases as FSD increases. This trend is physically expected in projection radiography because beam intensity at the skin decreases with increasing distance due to geometric divergence (the inverse square law dependence). For constant tube potential (kVp), the entrance-surface kerma is mainly governed by tube output proportional to mAs and by the distance factor $(SID/FSD)^2$; therefore, increasing FSD should reduce ESAK, consistent with the inverse square law [18].

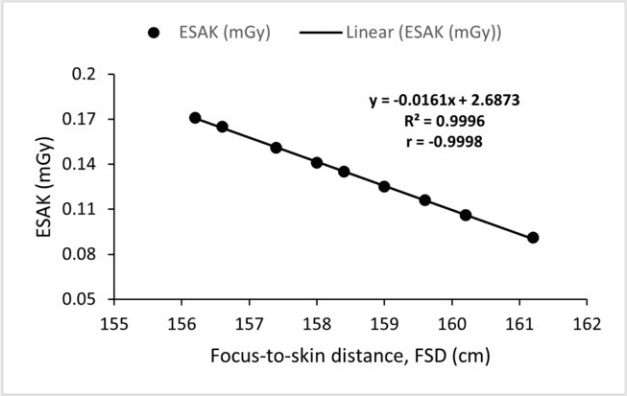

Figure 3. Correlation between ESAK and FSD.

However, the ESAK–FSD correlation in this dataset should be interpreted with caution because FSD is not an independent experimental variable. In routine PA chest radiography with a fixed SID, FSD is geometrically linked to patient habitus (e.g., chest thickness): an increase in thickness reduces FSD (a larger patient-to-detector gap) and simultaneously increases attenuation. As a result, AEC typically selects a higher mAs to maintain detector exposure. Because ESAK is calculated from tube output multiplied by mAs and corrected for distance (and backscatter), both mAs and the distance correction co-vary with patient thickness. Thus, the strong ESAK–FSD pattern is best understood as a combined consequence of (i) geometric distance effects and (ii) AEC-driven increases in mAs in thicker patients, rather than as a separable "distance-only" causal effect.

The fitted linear slope should therefore be interpreted as an empirical sensitivity within the limited observed range, not as a fundamental law. Moreover, the intercept of the linear fit should not be assigned physical meaning, because extrapolation beyond the measured FSD range is not valid; the intercept is a regression artifact from fitting a straight line to data generated by a multiplicative model (mAs × distance correction) over a restricted range.

Backscatter was included via a backscatter factor (BSF). Because exam-specific determinants of BSF (field size/collimation, HVL/filtration, etc.) were not fully available in routine records, a constant BSF was used as a pragmatic audit assumption. This introduces systematic uncertainty in absolute ESAK values, although the negative ESAK–FSD trend is expected to remain. Future work should record geometric details (patient-to-detector gap, actual FSD measurements) and technical parameters (collimation, HVL/filtration, AEC chamber selection, exposure index) to better separate the contributions of distance, technique (mAs), and scatter to dose variability.

3.4. Relationship between ESAK and Body Weight

Figure 4 shows the relationship between ESAK and body weight (BW). The linear model fitted to this dataset was:

$$ESAK = 0.00309 \cdot \mathrm{BW} - 0.05806 \tag{8}$$

and the result indicates a fairly strong association within this sample. Clinically, the direction of the relationship is plausible because higher body weight is often associated with greater attenuation, which can prompt the AEC to increase mAs to maintain detector exposure and thereby increase ESAK. In general, larger patient habitus leads to greater attenuation of the X-ray beam, reducing the detector signal for a given technique. In examinations performed with Automatic Exposure Control (AEC), increased attenuation may trigger the system to select a higher mAs to achieve the target receptor exposure and preserve image quality. Because the number of emitted photons is approximately proportional to mAs when kVp is held constant, this mechanism can contribute to higher incident air kerma (INAK) and, consequently, higher ESAK [13–14].

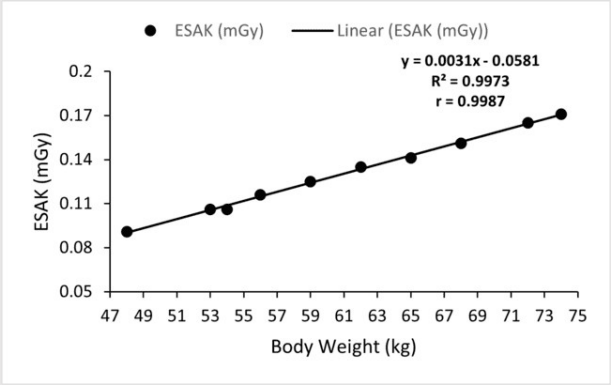

Figure 4. Correlation between ESAK and body weight.

However, the strength of this relationship should be interpreted cautiously. Body weight is not a direct measure of thoracic attenuation and is likely correlated with chest thickness. Chest thickness influences the mAs selected by the AEC and also affects the estimated FSD through Equation (1). Therefore, the observed ESAK–BW pattern may reflect these linked relationships rather than an independent effect of body weight alone.

Given the small sample size (n = 10) and relatively narrow ranges, the regression and correlation results are best treated as descriptive summaries of this dataset. Confirmation using a larger cohort and multivariable analysis that includes chest thickness, mAs, and estimated FSD simultaneously would be needed to better separate the contributions of patient habitus and technical factors.

3.5. Comparison with Reference Level and Optimization Implications

The mean ESAK in this pilot dataset was 0.13 mGy, with values ranging from 0.09 mGy to 0.17 mGy, and this was below the BAPETEN reference level or IDRL for adult PA chest radiography of 0.2 mGy [19]. This indicates that the ESAK values observed in this small sample are within the facility optimization benchmark context, rather than demonstrating a definitive facility wide performance or compliance status. Interpretation should remain cautious because the sample size is limited to 10 examinations and because ESAK estimation involved simplifying assumptions, particularly the use of a constant backscatter factor with BSF equal to 1.35 and the estimation of FSD from the fixed SID and recorded chest thickness.

The observed ESAK range is broadly consistent with reports from digital radiography studies in which adult PA chest ESAK commonly falls in the mGy range, while also emphasizing that dose levels are strongly

influenced by local technical and operational factors, including beam quality, examination geometry, detector characteristics, collimation or field size, and the specific dose metric applied [9,10]. Several studies in Indonesia have reported that ESAK variability is associated with exposure parameters and patient habitus, particularly through the AEC mechanism that modulates mAs under fixed kVp conditions [13,14]. However, in this study relationships involving mAs and FSD should be interpreted as expected consequences of the dose calculation model and AEC controlled exposure rather than as independent causal effects. In digital radiography, routine monitoring of exposure indicators such as exposure index alongside technique and geometry parameters is recommended to control variability and mitigate exposure creep [16,17]. Overall, the present results are best regarded as an initial local baseline to support subsequent audits using larger cohorts and more comprehensive parameter documentation, including field size or collimation, AEC chamber selection, grid use, filtration or HVL, exposure index, and positioning related patient to detector gap [13,17].

4. Conclusion

An observational descriptive exploratory pilot audit was performed on 10 adult PA chest radiographic examinations using a routine protocol with tube voltage fixed at 125 kVp and SID fixed at 180 cm. The estimated INAK ranged from 0.07 mGy to 0.13 mGy with a mean of 0.097 mGy, while the estimated ESAK ranged from 0.09 mGy to 0.17 mGy with a mean of 0.13 mGy, and ESAK was consistently higher than INAK because it includes backscatter. Within this dataset, variations in ESAK were consistent with differences in AEC selected mAs and with patient specific geometry represented by estimated FSD derived from SID and chest thickness, while higher body weight tended to coincide with higher mAs and higher ESAK. These patterns should be interpreted as descriptive and as expected sensitivity of the dose calculation model and AEC controlled exposure, rather than as independent causal effects. The mean ESAK in this pilot dataset was below the BAPETEN reference level or IDRL of 0.2 mGy, providing an initial facility baseline for optimization benchmarking. However, conclusions are limited by the small sample size, the use of a constant BSF, and incomplete documentation of key technical factors such as field size or collimation, filtration or HVL, grid use, AEC chamber selection, exposure index, and patient to detector gap. Future audits with larger cohorts and more complete parameter recording are recommended to strengthen local dose monitoring and optimization.

5. Acknowledgments

The authors express their sincere gratitude to colleagues at the Medical Physics and Nuclear Applications Laboratory, Universitas Syiah Kuala, for the academic and technical support provided throughout the course of this study. Appreciation is also extended to the Radiology Department of the hospital for granting permission and providing the opportunity to conduct observations and collect the data used in this research.

References

[1] S. Prabhu, D. K. Naveen, S. Bangera, and S. Bhat B, “Production of X-rays using X-ray tube,” *Journal of Physics: Conference Series*, vol. 1712, pp. 1-12, 2020.

[2] I. I. Suliman, “Estimates of Patient Radiation Doses in Digital Radiography Using DICOM Information at a Large Teaching Hospital in Oman,” *J Digit Imaging*, vol. 33, no.1, pp. 64-70, 2020. doi: 10.1007/s10278-019-00199-y.

[3] V. Tsapaki, “Radiation dose optimization in diagnostic and interventional radiology: Current issues and future perspectives,” *Physica Medica*, vol. 79, pp. 16–21, 2020. doi: 10.1016/j.ejmp.2020.09.015.

[4] Badan Pengawas Tenaga Nuklir (BAPETEN), *Peraturan Kepala Badan Pengawas Tenaga Nuklir Nomor 8 Tahun 2011 tentang Keselamatan Radiasi dalam Penggunaan Pesawat Sinar X Radiologi Diagnostik dan Intervensional*. Jakarta, Indonesia: BAPETEN, 2011. [Online]. Available: https://jdih.bapeten.go.id/unggah/dokumen/peraturan/81-full.pdf. [Accessed: Jan. 7, 2026].

[5] E. Vañó, D. L. Miller, C. J. Martin, M. M. Rehani, K. Kang, M. Rosenstein, P. Ortiz-López, S. Mattsson, R. Padovani, and A. Rogers, “Diagnostic Reference Levels in Medical Imaging, ICRP Publication 135,” *ICRP*, vol. 46, no. 1, pp. 1–144, 2017. doi: 10.1177/0146645317717209.

[6] International Atomic Energy Agency (IAEA), Dose Management Systems From Setting up to Quality Assurance,” IAEA Human Health Series No. 49, Vienna, Austria: IAEA, 2025. [Online]. https://www-pub.iaea.org/MTCD/publications/PDF/p15847-PUB2112_web.pdf. [Accessed: Jan. 7, 2026].

[7] I. I. Suliman, “An approach for the online determination of Entrance Surface Air Kerma (ESAK) from Kerma Area product (P_{KA}) in digital radiology,” *Phys Eng Sci Med*, vol. 45, pp. 1055-1061, 2022. doi: 10.1007/s13246-022-01167-7.

[8] C. Kaushik, I. S. Sandhu, A. K. Srivastava, and M. Chitkara, "Estimation of entrance surface air kerma in digital radiographic examinations," *Radiation Protection Dosimetry*, vol. 193, no. 1, pp. 16–23, 2021. doi:10.1093/rpd/ncab018.

[9] A. Promduang, N. Pongnapang, N. Ritlumlert, S. Tangruangkiat, and M. Phonlakrai, "A study of entrance surface air kerma for patients undergoing chest and abdomen from digital radiography at Chulabhorn Hospital," *Journal of Health Science and Medical Research*, vol. 37, no. 1, pp. 51–60, 2019.

[10] A. O. Masoud, M. J. Kumwenda, S. K. Salum, A. M. Jusabani, and K. O. Amour, "Radiation Doses to Patients Undergoing Common X-ray Examinations from Selected Hospitals in Dar es Salaam and Zanzibar, Tanzania," *Tanzania Journal of Science*, vol. 50, no. 3, pp. 569–579, 2024, doi:10.4314/tjs.v50i3.12.

[11] H. D. R. Raharja, N. I. S. Supit, and U. N. Haposan, "Estimasi dan audit dosis radiasi pasien pada pemeriksaan radiografi konvensional toraks PA dengan teknik high kVp," *Prosiding Seminar Si-INTAN*, Vol. 2, No. 1, 2022, pp. 63-68, doi:10.53862/SSI.v2.072022.010.

[12] A. Creeden and M. Curtis, "Optimising default radiographic exposure factors using deviation index," *Radiography*, vol. 26, no. 4, pp. 308–313, 2020. doi:10.1016/j.radi.2020.02.009.

[13] R. Putri, D. Milvita, and I. B. G. P. Pratama, "Analisis korelasi nilai entrance surface air kerma (ESAK) terhadap massa tubuh, usia, dan faktor eksposi pada pasien pemeriksaan radiografi umum di RSUP Dr. M. Djamil Padang," *Jurnal Fisika Unand*, vol. 14, no. 4, pp. 413–420, 2025. doi: 10.25077/jfu.14.4.413-420.2025

[14] S. I. Sari, D. Milvita, R. Fardela, I. B. G. P. Pratama, and A. Oktavia, "Analisis korelasi umur, massa tubuh dan faktor eksposi terhadap Entrance Surface Air Kerma pada pemeriksaan thorax di Rumah Sakit Universitas Andalas," *Jurnal Fisika Unand*, vol. 13, no. 5, pp. 602–609, 2024. doi:10.25077/jfu.13.5.602-609.2024.

[15] P. I. Wulandari, N. P. R. Jeniyanthi, I. M. L. Prasetya, I. P. A. Susanta, I. P. E. Juliantara, and A. A. Diartama, "Evaluasi dosis radiasi pada pemeriksaan radiografi thorax," *PREPOTIF: Jurnal Kesehatan Masyarakat*, vol. 7, no. 3, pp. 16325–16330, 2023. doi: 10.31004/prepotif.v7i3.19824.

[16] S. Lewis, T. Pieterse, and H. Lawrence, "Retrospective evaluation of exposure indicators: A pilot study of exposure technique in digital radiography," *Journal of Medical Radiation Sciences*, vol. 66, pp. 38–43, 2019.

[17] H. Park, J. Kim, E.-J. Kang, Y. Kim, H. Jo, J.-H. Heo, W. Yang, and Y. Yoon, "Feasibility of new patient dose management tool in digital radiography: Using clinical exposure index data of mobile chest radiography in a large university hospital," *Heliyon*, vol. 9, no. 10, 2023. doi: 10.1016/j.heliyon.2023.e20760.

[18] European Commission, *European Guidance on Estimating Population Doses from Medical X-Ray Procedures*, "Radiation Protection No. 154," Luxembourg: Directorate-General for Energy and Transport, Directorate H — Nuclear Energy, Unit H.4 — Radiation Protection, 2008. [Online]. https://www.sprmn.pt/pdf/RP154.pdf. [Accessed: Jan. 7, 2026].

[19] Badan Pengawas Tenaga Nuklir (BAPETEN), *Lampiran Keputusan Kepala Badan Pengawas Tenaga Nuklir Nomor 1812 Tahun 2025 tentang Penetapan Nilai Tingkat Panduan Diagnostik Indonesia (Indonesian Diagnostic Reference Level) untuk Pemeriksaan Pasien dengan Pesawat Sinar-X Radiografi Umum, CT-Scan, Fluoroskopi Intervensional, dan Pemeriksaan Kedokteran Nuklir Diagnostik*, Jakarta, Indonesia: BAPETEN, 2025. [Online]. https://bapeten.go.id/upload/78/84a27d22df-1812lampiransurat-keputusan-kepala-tentang-tpdi-2025.pdf. [Accessed: Jan. 7, 2026].

[20] International Atomic Energy Agency (IAEA), *Dosimetry in Diagnostic Radiology: An International Code of Practice*, IAEA Technical Reports Series No. 457, Vienna, Austria: IAEA, 2007. [Online]. https://www-pub.iaea.org/MTCD/Publications/PDF/TRS457_web.pdf. [Accessed: Jan. 7, 2026].